Atmospheric Available Energy

PETER R. BANNON

Department of Meteorology, The Pennsylvania State University, University Park, Pennsylvania

(Manuscript received 22 February 2012, in final form 4 June 2012)

ABSTRACT

The total potential energy of the atmosphere is the sum of its internal and gravitational energies. The portion of this total energy available to be converted into kinetic energy is determined relative to an isothermal, hydrostatic, equilibrium atmosphere that is convectively and dynamically "dead." The temperature of this equilibrium state is determined by minimization of a generalized Gibbs function defined between the atmosphere and its equilibrium. Thus, this function represents the maximum amount of total energy that can be converted into kinetic energy and, hence, the available energy of the atmosphere. This general approach includes the effects of terrain, moisture, and hydrometeors. Applications are presented for both individual soundings and idealized baroclinic zones. An algorithm partitions the available energy into available baroclinic and available convective energies. Estimates of the available energetics of the general circulation suggest that atmospheric motions are primarily driven by moist and dry fluxes of exergy from the earth's surface with an efficiency of about two-thirds.

1. Introduction

Lorenz (1955), building on the work of Margules (1910), formulated the concept of available potential energy (APE) as that portion of the total potential energy, that is, the sum of the gravitational and internal energy in hydrostatic balance, that is available for conversion into kinetic energy. Since then the concept has been a cornerstone of large-scale dynamic meteorology and the theory of the general circulation (e.g., Lorenz 1967; Peixoto and Oort 1991). The Lorenz formulation is a Lagrangian one that determines the APE for an isentropic rearrangement of air parcels. For an atmosphere that is statically stable, the entropy increases with height. Thus, an isentropic vertical rearrangement of the parcels is excluded and the theory only assesses the available energy associated with the leveling of isentropic layers toward geopotential surfaces. This feature is an ideal means to assess the energy available for conversion to kinetic energy by baroclinic instability processes. However, this feature precludes the theory from evaluating the energy available for a purely vertical (e.g., convective) rearrangement. The theory requires the specification of a reference state. For example, if the APE is defined on isobaric coordinates, a reference (potential) temperature must be assigned. The specification of the reference temperature remains an unsolved problem in the theory (e.g., Dutton and Johnson 1967; Lorenz 1979; Pauluis 2007). [Randall and Wang (1992) advance a numerical, parcel-moving algorithm to find the temperature structure for their generalized convective available potential energy (GCAPE) that is applied to a single atmospheric sounding.]

Eulerian formulations of the available energy have appeared in several formulations: entropic energy (Dutton 1973; Livezey and Dutton 1976), static exergy (Karlsson 1990), extended exergy (Kucharski 1997), and available energy (Bannon 2005). These formulations differ slightly in their base state and their treatment of water vapor and hydrometeors. They all require the specification of a reference temperature. Dutton (1973) uses a reference temperature defined from the total potential energy. Karlsson (1990) uses a reference temperature that minimizes the entropy difference between the atmosphere and its reference atmosphere. Kucharski (1997) uses a reference temperature profile based on the horizontally averaged density field.

The present work reexamines and refines the formulation of the Eulerian atmospheric available energy

Corresponding author address: Peter R. Bannon, Department of Meteorology, The Pennsylvania State University, University Park, PA 16802.
E-mail: bannon@ems.psu.edu

DOI: 10.1175/JAS-D-12-059.1

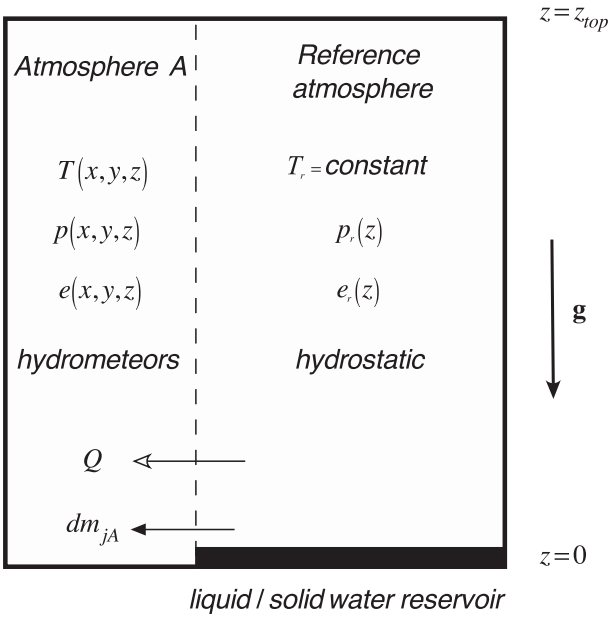

FIG. 1. Schematic diagram depicting an atmosphere A in thermal, mechanical, and diffusive contact with a hydrostatic, isothermal reference atmosphere. The reference surface vapor pressure is that for saturation at the temperature T_r for a reference atmosphere in contact with a water reservoir. The reference atmosphere is a dynamically and convectively ''dead'' state.

(AE) of Bannon (2005) that defines the available energy as a generalized Gibbs function between the atmosphere and an isothermal reference atmosphere at the temperature T_r. The reference atmosphere is in thermal and hydrostatic equilibrium (Fig. 1) and, hence, is dynamically and convectively ''dead.'' It has the same mass per unit area of dry air and water as the atmosphere. The reference temperature is determined uniquely by minimizing this function. Section 2 presents a thermodynamic proof that the maximum kinetic energy that can be extracted from the total energy is specified by the minimum of the generalized Gibbs function. Minimization is defined to occur at the isothermal reference temperature T_0. The outline of the proof follows but generalizes that in Reif (1965, section 8.3). Independently Karlsson (1990) suggested this minimization of his exergy formulation but did not pursue it. Section 3 describes the construct of the equilibrium atmosphere and the need for the careful treatment of the hydrometeors. Section 4 derives the governing equation for the evolution of the available energetics of a flow. The sources and sinks of AE are quantified as well as the partitioning of the AE into available potential and available elastic components. The positive definite nature of the AE is demonstrated along with its relation to the exergy approach of engineering thermodynamics (Bejan 1997). Section 5 presents some applications of AE to the standard atmosphere, idealized baroclinic zones, and observed moist soundings. It is demonstrated that the available energy shares properties with the Lorenz APE as well as convective available potential energy (CAPE). The available energy is partitioned into available baroclinic energy (ABE) and available convective energy (ACE) components. Section 6 estimates the available energetics of the general circulation.

2. Thermodynamic derivation of the atmospheric available energy

We consider the universe to be composed of a multicomponent system A and a large multicomponent reservoir, denoted with the subscripts A and res, respectively. The system is the atmosphere in thermal, mechanical, and diffusive contact with the reservoir that is a motionless reference atmosphere (see Fig. 1). State variables of the reference atmosphere are denoted for brevity with a subscript r. By the second law of thermodynamics, the entropy S of this universe tends to increase:

$$\Delta S = \Delta S_A + \Delta S_{\text{res}} \geq 0, \tag{2.1}$$

where Δ denotes a finite change between a final and initial state. For example, $\Delta S = S_{\text{final}} - S_{\text{initial}}$. The specific entropy can be determined from the general thermodynamic differential relation

$$du = Tds - pd\alpha + \mu_j d\chi_j, \tag{2.2}$$

where u is the specific internal energy, T is the temperature, s is the specific entropy, p is the pressure, and α is the specific volume. Here μ_j is the specific chemical potential of the jth component of mass m_j and χ_j is the concentration of the jth component (i.e., the mass of the jth component per total mass). The summation convention is assumed for repeated indices. A finite temporal change in the internal energy of the whole reservoir is

$$\Delta U_{\text{res}} = T_r \Delta S_{\text{res}} - W_{\text{res}} - M, \tag{2.3}$$

where $W_{\text{res}} = \int p_r \, dV_r$ is the total quasi-static pressure work done by the reservoir and $M = \int \mu_{rj} \, dm_{Aj}$ is the total transfer of Gibbs free energy due to the exchange of mass out of the reservoir into the system A. Here dm_{Aj} is the elemental mass of the jth component transferred out of the reservoir into the system A. The first law applied to the reference atmosphere is

$$\Delta U_{\text{res}} = -Q - W_{\text{res}}, \tag{2.4}$$

where Q is the thermal energy transferred out of the reservoir into the system A, including that due to mass exchange. The two relations (2.3) and (2.4) combine to express the temporal entropy change of the reservoir as

$$T_r \Delta S_{\text{res}} = -Q + M. \tag{2.5}$$

Then the total temporal entropy change is

$$\Delta S = \Delta S_A - \frac{Q}{T_r} + \frac{M}{T_r} \geq 0. \tag{2.6}$$

Solving this relation for the thermal energy transfer Q yields

$$Q = T_r \Delta S_A + M - T_r \Delta S. \tag{2.7}$$

The first law applied to the system A is

$$\Delta U_A = Q - W_A - W^*, \tag{2.8}$$

where $W_A = \int p_r \, dV_A$ is the total pressure work done by A on the reservoir with pressure p_r and W^* is any additional work done by A. In particular the additional work can represent the energy transfer into the kinetic energy of A. Eliminating the thermal energy transfer Q between (2.7) and (2.8) yields

$$\Delta G_A \equiv \Delta U_A - T_r \Delta S_A + W_A - M = -T_r \Delta S - W^*, \tag{2.9}$$

where ΔG_A is defined as a finite temporal change in the generalized Gibbs function G_A of the atmosphere A at the reference temperature, pressure, and chemical potential of the reservoir. Then the total entropy change is

$$\Delta S = \left(\frac{-\Delta G_A - W^*}{T_r} \right) \geq 0. \tag{2.10}$$

This inequality implies that any additional work W^* done by A requires a decrease in its Gibbs function with time:

$$\Delta G_A \leq -W^*. \tag{2.11}$$

If $W^* = 0$, then $\Delta G_A \leq 0$ and the equilibrium state of the atmosphere in which no more work can be done satisfies the condition that G_A tends to a minimum with time.

We assume that the atmosphere A can obtain its reference state and define its Gibbs function in that state as G_{Ar}. Then the finite difference in the Gibbs functions between that of the atmosphere and that of the reference state may be defined as $\delta G_A \equiv G_A - G_{Ar} > 0$. [The symbol δ defines a finite difference between A and its reference state. In contrast, ΔG_A denotes the finite change with time of the atmosphere's Gibb function and, by (2.11), is negative as the atmosphere tends to an equilibrium.] Because the system A is not necessarily in the equilibrium state, $\delta G_A > 0$ in general but A will be in equilibrium with $W^* = 0$ when δG_A is a minimum. The novel feature here is that we seek to determine the reference temperature T_r that minimizes δG_A (typically the reference quantities are specified a priori by, say, the laboratory setting or the environment). Figure 2 provides an example. At the reference temperature $T_r = T_0$, the change in the Gibbs function is a minimum $\delta G_{\min}$. If we take the additional work W^* to be the increase in the kinetic energy KE* of the system A, then the inequality (2.10) becomes

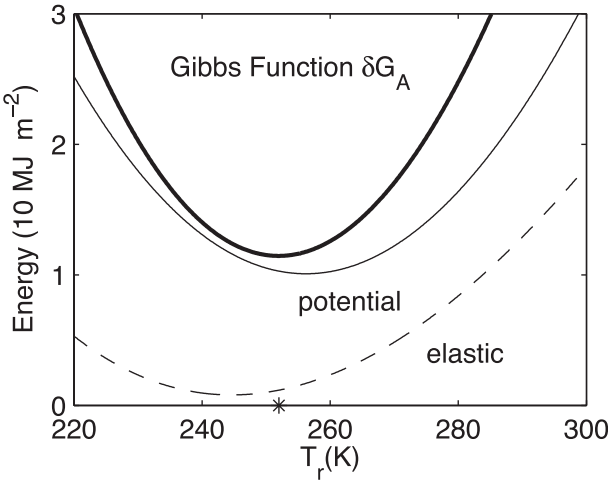

FIG. 2. The atmospheric Gibbs function δG_A for a 25-km-deep standard atmosphere as a function of the reference temperature T_r. This function, denoted by the heavy solid curve, has a minimum at the equilibrium temperature, denoted by the asterisk on the abscissa, of $T_0 = 251.95$ K. The solid and dashed curves denote the potential and elastic contributions to this function, respectively, defined in section 4b.

$$\text{KE}^* = \delta G_{\min} - T_r \delta S \leq \delta G_{\min}. \tag{2.12}$$

The maximum possible increase in kinetic energy is that for the reversible case ($\delta S = 0$)

$$\text{KE}^*_{\max} = \delta G_{\min} \equiv \text{AE} > 0, \tag{2.13}$$

where the available energy AE is the maximum energy available to be converted into kinetic energy.

This procedure has enabled the available energy of the atmosphere to be expressed in terms of a generalized Gibbs function defined in terms of the temperature,

pressure, and chemical potentials of its equilibrium state. The specific available energy is, from (2.9) and dropping the subscript A,

$$\text{ae} = \delta u - T_0 \delta s + p_0 \delta\alpha - \mu_{oj}\delta\chi_j. \tag{2.14}$$

It proves convenient to rewrite this expression in terms of the specific enthalpy $h = u + p\alpha$. Then $\delta u = \delta h - \delta(p\alpha) = \delta h - p\delta\alpha - \alpha_0\delta p$ and the available energy is

$$\text{AE} = \int \text{ae}\, dm, \tag{2.15}$$

where $\text{ae} = \delta h - T_0\delta s - \alpha\delta p - \mu_{0j}\delta\chi_j$. Here a subscript 0 refers to the equilibrium temperature that minimizes the function δG_A of the system. Unsubscripted variables are functions of position $\mathbf{x} = (x, y, z)$ and time t but the equilibrium entropy, pressure, and chemical potentials are only functions of height z. Again, the symbol δ defines a finite departure of the atmosphere from its equilibrium state. For example, $\delta h = h(\mathbf{x}, t) - h_0(z)$.

3. Specification of the equilibrium state

The atmosphere and its equilibrium are henceforth taken to be of fixed volume. The equilibrium atmosphere is isothermal and hydrostatic at the temperature T_0. Then, the dry air and vapor pressures are, in a Cartesian geometry,

$$p_0 = p_* \exp\left(-\frac{z}{H_s}\right), \quad e_0 = e_* \exp\left(-\frac{z}{H_{sv}}\right), \tag{3.1}$$

where the asterisks denote a surface ($z = 0$) value and the scale heights are $H_s = R_d T_0/g$ and $H_{sv} = R_v T_0/g$ (details of the thermodynamic formulations and the values of physical constants are summarized in appendix A). In order that the equilibrium state has the same mass per unit area of dry air M_d and water vapor M_v as atmosphere A, the surface pressures are

$$p_* = \left[\frac{gM_d}{1 - \exp(-z_{\text{top}}/H_s)}\right], \quad e_* = \left[\frac{gM_v}{1 - \exp(-z_{\text{top}}/H_{sv})}\right], \tag{3.2}$$

where the exponential factor accounts for the finite height z_{top} of the atmosphere (Fig. 1). If topography is present, (3.2) is modified in a straightforward manner to conserve mass between A and its equilibrium atmosphere. If the surface vapor pressure e_* is greater than the saturation vapor pressure at the temperature T_0, then e_* is set to that of saturation and an amount P of water per unit area has precipitated into the water reservoir (Fig. 1),

$$e_* = e_{\text{sat}}(T_0) \quad \text{and} \quad P = M_v - M_{v0}. \tag{3.3}$$

Then the amount of water vapor in the equilibrium state becomes

$$M_{v0} = \frac{e_{\text{sat}}(T_0)}{g}[1 - \exp(-z_{\text{top}}/H_{sv})]. \tag{3.4}$$

It is instructive to examine the consequences of the application of the available energy (2.14) for a fixed volume of dry air only. Then (2.15) with (2.14) becomes

$$\text{AE} = \int_V \rho\,\text{ae}\, dV, \tag{3.5}$$

where $\text{ae} = \delta u - T_0\delta s + p_0\delta\alpha$. The last term vanishes when integrated over the fixed volume because of mass conservation:

$$\int \rho p_0 \delta\alpha\, dV = R_d T_0 \int \rho\rho_0(\alpha - \alpha_0)\, dV = R_d T_0 \int (\rho_0 - \rho)\, dV = 0. \tag{3.6}$$

Then the available energy is the Helmholtz free energy.

The expression for the available energy also requires the equilibrium chemical potentials. We adopt the convention that the subscripts $j = 1$ and 2 refer to the dry air and water vapor, respectively, and the subscripts $j = 3$ and 4 refer to liquid water and ice. For a gas we have

$$\mu_{0j} = h_j - T_0 s_j = c_{pj}(T_0 - T_c) - T_0\left[c_{pj}\ln\left(\frac{T_0}{T_c}\right) - R_j \ln\left(\frac{p_0}{p_c}\right)\right], \tag{3.7}$$

where the quantities with subscript c are arbitrary constants that do not affect the computations. Because of the exponential decay of the gas pressures with height (3.1), the chemical potentials of dry air and water vapor decrease linearly with height ($\mu_j = -gz + \text{const}$). In contrast, the chemical potentials for liquid and solid water contain no pressure terms and would be independent of height.

This asymmetry is physically appropriate for the equilibrium atmosphere. The criterion (Gibbs 1873, 1874, p. 146) for equilibrium of a system in a gravitational field

is that the total chemical potential (i.e., the sum of the intrinsic chemical potential μ and the geopotential gz) is constant. The expression (3.7) for the dry air and water vapor satisfies this criterion. In contrast, the total potentials for the hydrometeors are not constant and these components are not in equilibrium. This disequilibrium is physically correct because all hydrometeors have nonzero terminal fall speeds and will eventually settle out.

In practice it has proven convenient a posteriori to include a geopotential contribution to the chemical potentials of the hydrometeors. Specifically the potentials for liquid and solid water are adjusted to have the same height dependence as the gases:

$$\mu_{0j} = h_j - T_o s_j - gz = c_j(T_0 - T_c) - T_0 c_j \ln\left(\frac{T_0}{T_c}\right) - gz. \tag{3.8}$$

This adjustment ensures that a phase change at a height $z > 0$ produces no superfluous accounting changes in the entropy and potential energy budgets. The derivation of the next section uses (3.8). Appendix B shows that the consequences of omitting the geopotential in (3.8) lead to an equivalent result.

4. Available energetics

This section uses a fluid dynamical approach to generalize the thermodynamic derivation of section 2 to include diabatic and frictional processes for an open atmosphere. It also quantifies the sources and sinks of the available energy and resolves issues related to the asymmetry in the chemical potentials discussed in section 3.

a. General derivation of the governing equation

This section presents a general derivation of the available energetics for a multicomponent, compressible fluid. The specific available energy, ae, is

$$\text{ae} = \delta h - T_0 \delta s - \alpha \delta p - \mu_{0,j} \delta \chi_j. \tag{4.1}$$

Its rate of change following the three-dimensional, mass-weighted, mean velocity $\mathbf{v}$ is

$$\begin{aligned}\frac{D}{Dt}\text{ae} = {} & \frac{Dh}{Dt} - T_0\frac{Ds}{Dt} - \frac{D(\alpha\delta p)}{Dt} - \frac{D}{Dt}(\mu_{0,j}\delta\chi_j) - \mu_{0,j}\frac{D}{Dt}\chi_{0,j} \\ & - \left[\frac{Dh_0}{Dt} - T_0\frac{Ds_0}{Dt} - \alpha_0\frac{Dp_0}{Dt} - \mu_{0,j}\frac{D}{Dt}\chi_{0,j}\right] \\ & - \alpha_0\frac{Dp_0}{Dt},\end{aligned} \tag{4.2}$$

where the material derivative is

$$\frac{D}{Dt} = \frac{\partial}{\partial t} + \mathbf{v}\cdot\nabla,$$

and $\mathbf{v} = \chi_j \mathbf{v}_j$ and $\chi_j = m_j/\sum_j m_j$, where m_j and $\mathbf{v}_j$ are the mass and velocity of the jth component. Then the continuity equation is

$$\frac{D\rho}{Dt} = -\rho\nabla\cdot\mathbf{v} \quad \text{or} \quad \frac{D\alpha}{Dt} = \alpha\nabla\cdot\mathbf{v}, \tag{4.3}$$

where ρ is the total density. For the hydrostatic equilibrium state, the force balance is

$$0 = -\nabla p_0 - \rho_0 \nabla\Phi \quad \text{or} \quad \alpha_0 \nabla p_0 = -\nabla\Phi, \tag{4.4}$$

where Φ is the geopotential. The Gibbs relation in the form $dh = Tds + \alpha dp + \mu_j d\chi_j$ for the equilibrium state implies that the term in square brackets in (4.2) vanishes. Then, using (4.3) and (4.4), (4.2) becomes

$$\begin{aligned}\frac{D\text{ae}}{Dt} = {} & \left(\frac{Dh}{Dt} - \alpha\frac{Dp}{Dt}\right) - \left(T_0\frac{Ds}{Dt} + \mu_{0,j}\frac{D}{Dt}\chi_j\right) \\ & + \left(\frac{D\Phi}{Dt} + \alpha\mathbf{v}\cdot\nabla p\right) - \alpha\nabla\cdot(\delta p\mathbf{v}) - \delta\chi_j\frac{D}{Dt}\mu_{0,j}.\end{aligned} \tag{4.5}$$

The last term vanishes because the material derivatives of the chemical potentials only contain a gravity contribution and the sum of the differences in concentrations vanish:

$$\left[-\delta\chi_j D\mu_{0,j}/Dt = gw\sum_j(\chi_j - \chi_{0,j}) = gw(1-1) = 0\right].$$

This result is a consequence of (3.8) that includes a gravity component to the chemical potentials of the hydrometeors. This assumption is addressed further in appendix B. The specific kinetic energy, ke, and enthalpy equations are

$$\frac{D\text{ke}}{Dt} = -\alpha\mathbf{v}\cdot\nabla p - \mathbf{v}\cdot\nabla\Phi + \alpha\mathbf{v}\cdot(\nabla\cdot\tau), \tag{4.6}$$

$$\frac{Dh}{Dt} = \alpha\frac{Dp}{Dt} + T\frac{Ds}{Dt} + \mu_j\frac{D\chi_j}{Dt}, \tag{4.7}$$

where τ is the viscous stress tensor. Then (4.5), (4.6), and (4.7) sum to give

$$\frac{D(\text{ae}+\text{ke})}{Dt} = \delta T\frac{Ds}{Dt} + \delta\mu_j\frac{D\chi_j}{Dt} + \alpha\mathbf{v}\cdot(\nabla\cdot\tau) - \alpha\nabla\cdot(\delta p\mathbf{v}). \tag{4.8}$$

The equation for the concentration rate of change is

$$\rho\frac{D\chi_j}{Dt}=\rho\dot{\chi}_j=-\nabla\cdot(\rho_j\mathbf{v}_j')+\dot{r}_j, \tag{4.9}$$

where ρ_j is the density of the jth component, whose velocity relative to the mass-weighted average velocity $\mathbf{v}$ is $\mathbf{v}_j'$ and whose rate of production by chemical reactions and/or phase changes is $\dot{r}_j$. The entropy equation is

$$\rho T\frac{Ds}{Dt}=\rho T\dot{s}=\rho\dot{q}+\rho\phi-\rho\mu_j\dot{\chi}_j, \tag{4.10}$$

where $\dot{q}$ is the heating rate due to radiation, conduction, and diffusion (i.e., the convergence of the enthalpy flux of the components with enthalpy h_j relative to the mean velocity). Here $\phi=\tau_{ij}e_{ij}>0$ is the viscous dissipation and e_{ij} is the rate of strain tensor. Then, the available energetics equation becomes

$$\rho\frac{D(\mathrm{ae}+\mathrm{ke})}{Dt}=-\nabla\cdot(\delta p\mathbf{v})+\nabla\cdot(\mathbf{v}\cdot\tau)+\rho\mathrm{sae}. \tag{4.11}$$

The internal sources of available energy are given by the last term in (4.11), where

$$\mathrm{sae}=\frac{\delta T}{T}\dot{q}-\frac{T_0}{T}\phi+T_0\left(\frac{\mu_j}{T}-\frac{\mu_{0,j}}{T_0}\right)\dot{\chi}_j \tag{4.12}$$

or, using the definition of the chemical potentials,

$$\mathrm{sae}=\frac{\delta T}{T}\dot{q}-\frac{T_0}{T}\phi-T_0(s_j-s_{0,j})\dot{\chi}_j. \tag{4.13}$$

For example, in the case of a phase change between water vapor and liquid water, we have

$$\mathrm{sae}_{\mathrm{phase}}=-T_0(s_j-s_{0,j})\dot{r}_j=-T_0R_v\ln H\dot{r}_2, \tag{4.14}$$

where H is the relative humidity. Thus, inclusion of the geopotential term in the equilibrium chemical potential for the hydrometeors (3.8) correctly handles entropy production during phase changes.

It is of some interest to compare the available energy defined here with the engineering concept of exergy (e.g., Bejan 1997). Typically the exergy of the jth component is $\mathrm{ex}_j=\delta h_j-T_0\delta s_j$ (plus Φ_j for the hydrometeors). Then the available energy may be written in terms of the exergy as $\rho\mathrm{ae}=\rho_j\mathrm{ex}_j-\delta p$ or $\mathrm{ae}=\mathrm{ex}-\alpha\delta p$ and the flux form of (4.11) is

$$\frac{\partial\rho(\mathrm{ae}+\mathrm{ke})}{\partial t}=-\nabla\cdot[\rho(\mathrm{ke}+\mathrm{ex})\mathbf{v}]+\nabla\cdot(\mathbf{v}\cdot\tau)+\rho\mathrm{sae}, \tag{4.15}$$

where the rate of working by the pressure field has dropped from the equation.

b. Partitioning and linearization of the available energy

The available energy (4.1) can be partitioned into the sum of the available energies of each component. Using relations of the form $\delta h=h-h_0$, $h=\chi_jh_j$, and $\mu=h-Ts$ yields $\rho\mathrm{ae}=\rho_j\mathrm{ae}_j$. The available energy ae_j for each component is now shown to be a positive definite quantity.

The available energy for dry air and water vapor ($j=1, 2$) may be partitioned (e.g., Bannon 2005) into available potential and available elastic contributions:

$$\mathrm{ae}_j=\delta h_j-T_0\delta s_j-\alpha_j\delta p_j=\mathrm{ape}_j+\mathrm{aee}_j, \tag{4.16}$$

where

$$\begin{aligned}\mathrm{ape}_j&=h_j(s,p_0)-h_j(s_0,p_0)-T_0\delta s_j\\&=c_{pj}T_0[\delta\hat{\theta}_j-\ln(1+\delta\hat{\theta}_j)]\simeq\frac{1}{2}c_{pj}T_0(\delta\hat{\theta}_j)^2,\end{aligned} \tag{4.17}$$

and

$$\begin{aligned}\mathrm{aee}_j&=h_j(s,p)-h_j(s,p_0)-\alpha_j\delta p_j\\&=c_{pj}T\left[1-\left(\frac{p_{0,j}}{p_j}\right)^{\kappa_j}-\kappa_j\delta\hat{p}_j\right]\simeq\frac{1}{2}\kappa_jc_{vj}T(\delta\hat{p}_j)^2.\end{aligned} \tag{4.18}$$

The specific entropy is $s=c_p\ln\theta$, where the potential temperature is $\theta_j=T(p_{00}/p_j)^{\kappa_j}$ with $\kappa_j=R_j/c_{pj}$ and the caret indicates a normalized departure. The equilibrium potential temperature normalizes the potential temperature departure $\delta\hat{\theta}_j=\delta\theta_j/\theta_{0,j}$, while the pressure normalizes the pressure departure $\delta\hat{p}_j=\delta p_j/p_j$.

The available energy for liquid or solid water ($j=3$ or 4) is

$$\begin{aligned}\mathrm{ae}_j&=\delta h_j-T_0\delta s_j+\Phi_j\\&=c_jT_0[\delta\hat{T}-\ln(1+\delta\hat{T})]+\Phi_j\simeq\frac{1}{2}c_jT_0(\delta\hat{T})^2+\Phi_j,\end{aligned} \tag{4.19}$$

where the geopotential $\Phi_j=gz$ arises from the definition (3.8). The equilibrium temperature normalizes the temperature departure $\delta\hat{T}=\delta T/T_0$. The expressions for the gases correctly reduce to those for a solid or liquid by taking $\kappa=0$.

The preceding formulas emphasize the enthalpic nature of the available energy. Their definitions in terms of

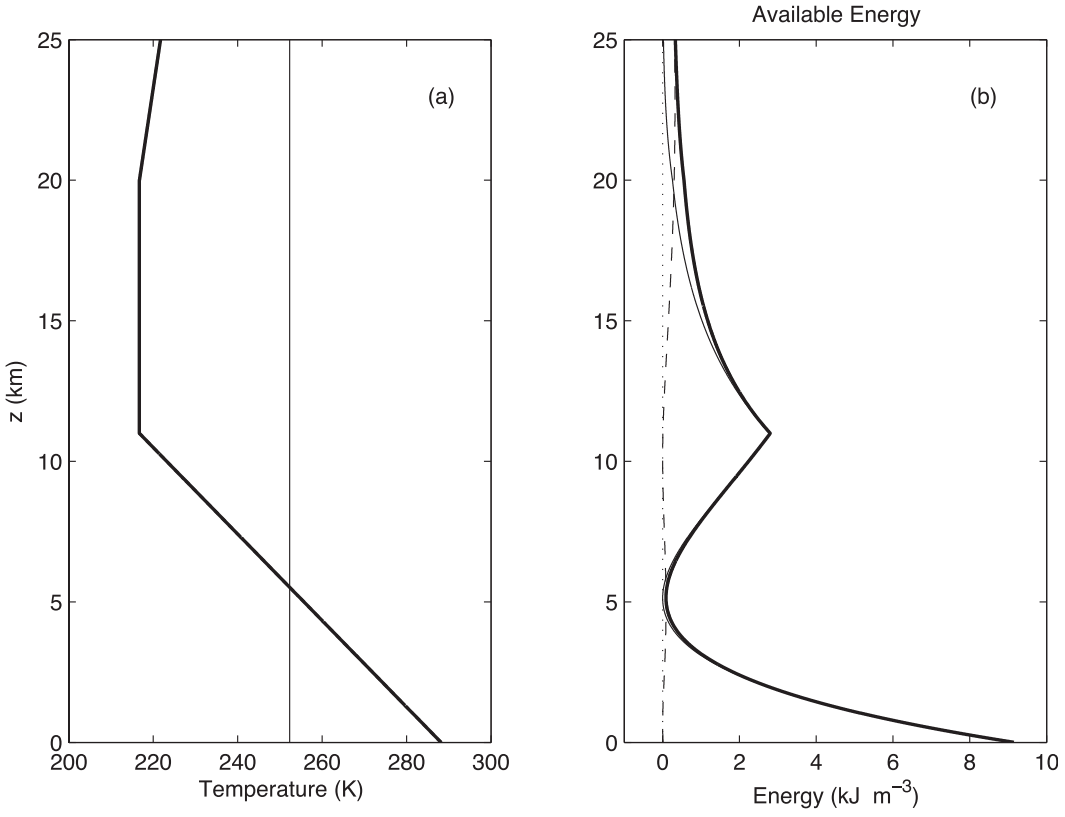

FIG. 3. (a) Temperature and (b) available energy as a function of height z for a 25-km-deep standard atmosphere. In (a) the thick solid and solid curves are the soundings for the atmosphere and its equilibrium atmosphere, respectively, with $T_0 = 251.95$ K. In (b) the solid, dashed, and thick solid curves denote the potential, elastic, and total contributions. The dotted vertical line is the zero line.

normalized departures are computationally advantageous to ensure positive definite calculations as well as providing easy derivations of their quadratic nature.

5. Applications

The available energy formalism is applied to several atmospheres to determine their equilibrium temperature T_0 and associated available energy.

a. Standard atmosphere

The case of the standard atmosphere in Fig. 2 is an example of the minimization of the atmospheric Gibbs function δG_A. This hydrostatic atmosphere extends to a height of 25 km with a surface temperature and pressure of 288.15 K and 1013.25 hPa. The lapse rates are 6.5, 0, −1.0, and −2.8 K km^{-1} for $z < 11$, 20, 32, and 50 km, respectively. The potential and elastic contributions are defined by (4.17) and (4.18). The temperature profile is plotted in Fig. 3a, where it is compared to its equilibrium temperature $T_0 = 251.95$ K. The total energy (TE) is slightly greater than that of its equilibrium atmosphere for both the 25- and 50-km-deep cases (Table 1). The internal energy (IE = U) differences between the atmosphere and its equilibrium are small and change sign between the two cases. For both, the potential energy (PE) is less for the equilibrium atmosphere. This reduction in PE is consistent with a lower center of gravity associated with the lower temperature of the equilibrium atmosphere in the lower troposphere (Fig. 3a). Because of the finite vertical extent of each atmosphere, the ratio of the potential to internal energy is

TABLE 1. Traditional energetics of two standard atmospheres of different depths. Values for the equilibrium atmosphere are in parentheses. The total energy is the sum of the internal and potential energies (TE = IE + PE).

Depth (km)	TE (GJ m^{-2})	IE (GJ m^{-2})	PE (GJ m^{-2})
25	2.4733 (2.4619)	1.8111 (1.8195)	0.6622 (0.6423)
50	2.5896 (2.5772)	1.8521 (1.8443)	0.7375 (0.7329)

TABLE 2. Available energetics of the two standard atmospheres. δTE is the difference of the total energies of the atmosphere and its equilibrium atmosphere.

Depth (km)	T_0 (K)	δTE (MJ m^{-2})	AE (MJ m^{-2})	APE (MJ m^{-2})	AEE (MJ m^{-2})
25	251.95	11.40	11.45	10.29	1.16
50	249.25	12.38	12.55	10.74	1.81

TABLE 3. Available energetics of the idealized baroclinic zone as a function of horizontal temperature gradient ΔT_y with no surface winds.

ΔT_y (K)	T_0 (K)	δTE (MJ m^{-2})	AE (MJ m^{-2})	APE (MJ m^{-2})	AEE (MJ m^{-2})
60	259.11	10.91	10.88	10.24	0.64
40	259.73	8.74	8.73	8.38	0.35
20	260.10	7.45	7.45	7.27	0.18
0	260.22	7.04	7.02	6.90	0.12

less than that of $R/c_{va} = 40\%$. Thus, the total energy is only approximately the enthalpy (cf. Lorenz 1955).

The available energy (AE) for both atmospheres resides primarily (Table 2) in the available potential energy (APE) with about 10% in the available elastic energy (AEE). For the 25 km deep atmosphere, the available energy of 11.45 MJ m^{-2} is much less than its total energy (Table 1) of 2.4733 GJ m^{-2}. Thus, only 0.46% is available for conversion into kinetic energy; 0.48% for the 50 km deep atmosphere. In contrast the available energy agrees well with the difference in total energy δTE between the atmosphere and its equilibrium state. This important feature indicates that, in achieving its equilibrium state, the atmosphere's total energy is reduced by an amount AE that can, in principle, be realized as kinetic energy. In this subsection and the next, the equilibrium temperature is determined to within an accuracy of 0.01 K so as to confirm the agreement between the change in total energy and the available energy. Elsewhere an accuracy of 0.1 K is used.

The vertical distribution of the available energy (Fig. 3b) is bimodal with a maximum at the surface, a secondary maximum at the tropopause, and a midtropospheric minimum near where the equilibrium temperature and the sounding (Fig. 3a) intersect. The secondary peak lies at the height of the change in the lapse rate. The elastic energy is significant in the stratosphere and its contribution dominates that of the potential energy above 20 km. This behavior holds for all of the cases analyzed and reflects that the elastic energy (4.18) is inversely proportional to the square of the pressure field.

b. Idealized baroclinic zones

The idealized baroclinic zones are based on a generalized compressible Eady base state (appendix C). The available energetics is summarized in Table 3 as a function of the total meridional temperature gradient ΔT_y. The results display a clear monotonic trend in all variables. As the amplitude of the baroclinity (ΔT_y) increases, the available energies AE, APE, and AEE increase, while the equilibrium temperature (T_0) decreases slightly. For each case, the difference in total energy between the atmosphere and its equilibrium state is the available energy.

The spatial variation of the available energy (Fig. 4a) exhibits a bimodal variation with larger values where the difference between the temperature and the equilibrium temperature is larger. The dominance of the temperature variation, rather than pressure variation, reflects the dominance of the available potential energy contribution (4.17) to the total available energy. The efficiency factor $N \equiv (T - T_0)/T$ also reflects this distribution (Fig. 4b). The abrupt transition at 11 km reflects the change to a zero lapse rate in the lower stratosphere.

The effect of a surface pressure gradient associated with a mean geostrophic wind is small (Table 4) with a slight increase in available energy as the wind transitions from westerly to easterly. Henceforth, the surface wind is set to zero.

The effect of sloping topography on the available energy is readily included in this Eulerian formulation. Table 5 provides a comparison for topography sloping linearly upward toward the pole (henceforth poleward) or toward the equator (henceforth equatorward) to reach a maximum height of 3 km (appendix C). The poleward case contains more available energy. This result is consistent with the linear Eady model analysis of Mechoso (1980) that indicates greater growth rates for unstable baroclinic waves for terrain sloping with the isentropes.

The effect of the inclusion of a moist boundary layer (appendix C) on the available energy is summarized in Table 6. The vapor pressure has a surface relative humidity of 70% and decays vertically with a scale height of 3 km. Inclusion of moisture has increased the equilibrium temperature by ~5 K to 265.12 K and increased all available energy components of the dry air. The vapor contributes to the available energy primarily through its elastic component. The distribution of the available energy and the efficiency factor (not shown) is similar to that of Fig. 4 for the dry case. The major effect of the moisture is through the increased equilibrium temperature that moves the zero efficiency isopleth downward. Figure 5 illustrates the

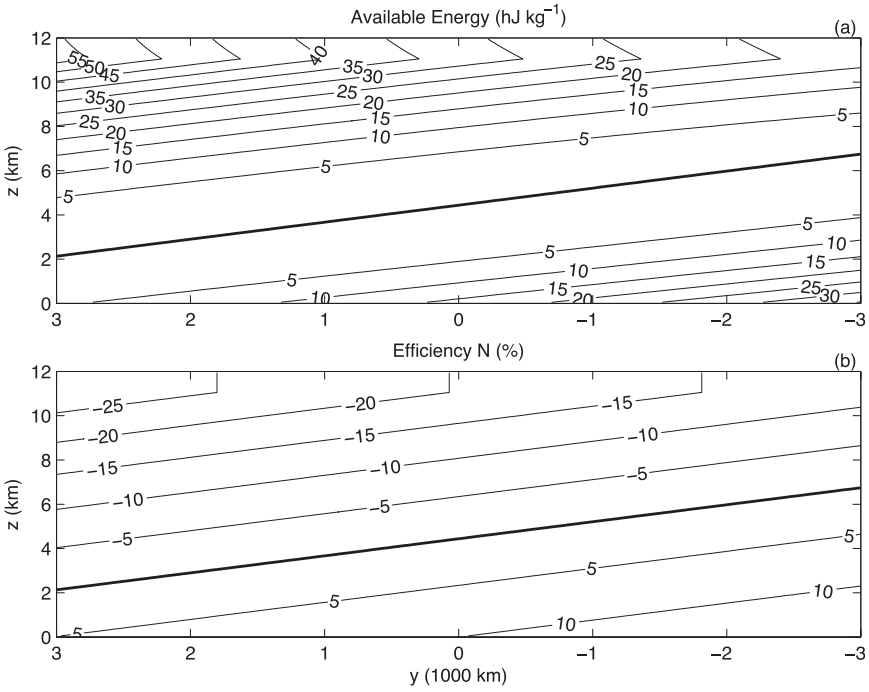

FIG. 4. Cross section of the (a) specific available energy and (b) the efficiency factor $N = (T - T_0)/T$ for the idealized baroclinic zone with $\Delta T_y = 30$ K. In each panel, the thick solid line is the zero efficiency isopleth.

effects of water vapor on the minimization of the Gibbs function. For reference temperatures below about 270 K, the reference atmosphere contains an ice reservoir of tens of kilograms per square meter of water. The enthalpy change associated with this phase transformation increases the Gibbs function curve at those temperatures and moves the temperature minimum toward warmer temperatures. The equilibrium atmosphere is saturated with an ice reservoir that is 1.29 cm thick due to precipitation (3.3). The ice contributes the major amount of the difference in total energy between the atmosphere and its equilibrium by its enthalpy of deposition (Table 6). The vertical distributions of the available energies (not shown) are similar to those presented in section 5d, which analyzes observed moist atmospheric soundings.

c. *Comparison with the available potential energy of Lorenz*

The evaluation of the available potential energy (LAPE) of Lorenz (1955) uses the approximate formula [Lorenz 1955, (10)]

$$\mathrm{LAPE} \approx \frac{1}{2}\int_{p_{\mathrm{top}}}^{1000\mathrm{hPa}} \frac{\overline{T}}{(\Gamma_d - \overline{\Gamma})}\overline{\left[\left(\frac{T'}{\overline{T}^2}\right)^2\right]}\, dp, \quad (5.1)$$

where an overbar denotes a horizontal average and a prime the deviation from that average. The LAPE is identically zero in the preceding horizontally homogeneous situations of section 5a. No adjustment is made here in the calculation of LAPE for isentropes intersecting the surface.

TABLE 4. Available energetics of the idealized baroclinic zone with $\Delta T_y = 30$ K and a surface pressure gradient Δp_y associated with a uniform geostrophic wind with a speed of 10 m s^{-1}.

Surface wind	T_0 (K)	δTE (MJ m^{-2})	AE (MJ m^{-2})	APE (MJ m^{-2})	AEE (MJ m^{-2})
Westerly	260.13	7.96	7.93	7.41	0.53
Calm	259.95	7.96	7.98	7.74	0.25
Easterly	259.71	8.34	8.32	8.15	0.17

TABLE 5. Available energetics of the idealized baroclinic zones over topography sloping upward toward the pole or toward the equator. The horizontal temperature gradient is $\Delta T_y = 30$ K. The total change in topography is 3 km.

Mountain	T_0 (K)	δTE (MJ m^{-2})	AE (MJ m^{-2})	APE (MJ m^{-2})	AEE (MJ m^{-2})
Poleward	254.75	6.24	6.23	6.03	0.20
Equatorward	252.52	4.81	4.82	4.63	0.19

TABLE 6. Available energetics of the moist idealized baroclinic zone with $\Delta T_y = 30$ K. The equilibrium temperature is $T_0 = 265.12$ K with a saturated surface vapor pressure of $e_* = 3.09$ hPa. The ice reservoir is 1.29 cm thick and contributes 30.18 MJ m^{-2} to the total energy difference.

Component	δTE (MJ m^{-2})	AE (MJ m^{-2})	APE (MJ m^{-2})	AEE (MJ m^{-2})
Dry air	−25.22	8.31	7.85	0.46
Water vapor	5.26	1.85	0.39	1.46
Total	10.21	10.17	8.25	1.92

Exact specification of the counterpart to the Lorenz APE in the present approach is thwarted by its nonlinear structure. For definiteness, the available energy of a single atmospheric sounding is defined as available convective energy (ACE). In contrast, the available baroclinic energy (ABE) is defined as the amount of available energy in excess of that needed to bring the system to the lowest equilibrium temperature $T_{\min}$ of the individual soundings in the ensemble of soundings. Then,

$$\mathrm{ABE} = \delta G_A(T_{\min}) - \delta G_A(T_0), \tag{5.2}$$

where $\mathrm{AE} = \delta G_A(T_0)$. Conceptually this approach views the determination of the ABE as a two-step process in which the atmosphere collectively adjusts *vertically* to its state of lowest total energy. A subsequent adjustment of the system then occurs *laterally* among the columns to the equilibrium temperature T_0. Alternatively, the atmosphere could first adjust to the temperature of the sounding with the warmest ACE temperature $T_{\max}$. Graphically (Fig. 5) the minimum and maximum temperatures straddle T_0. The difference in the values of the ABE estimated by the two approaches reflects the asymmetry of the parabolic shape of the atmospheric Gibbs function about T_0. The results (Table 7) indicate qualitative agreement between the ABE and LAPE values. The available baroclinic energy increases with the inclusion of moisture and with topography sloping against the slope of the isotherms. In all cases, the LAPE is less than the AE. This inequality indicates that the Lorenz formulation underestimates the amount of available energy.

d. Individual moist soundings

A real data case is afforded by the sounding from the Second Verification of the Origins of Rotation in Tornadoes Experiment [VORTEX2; 2155 UTC 5 June 2009, National Severe Storms Laboratory (NSSL1)] presented in Fig. 6. The sounding exhibits a large potential for deep convection for parcels ascending above about 700 hPa along the 70°C saturated adiabat. The convective available potential energy (CAPE) evaluated from 700 to 170 hPa is 2370 J kg^{-1}. Assuming hydrostatic balance, the available energy may be analyzed in pressure coordinates. The minimization of the atmospheric Gibbs function (not shown) is similar to that depicted in Fig. 5. Table 8 and Fig. 7 present the results of an AE analysis of the profile. The dry air AE (Fig. 7a)

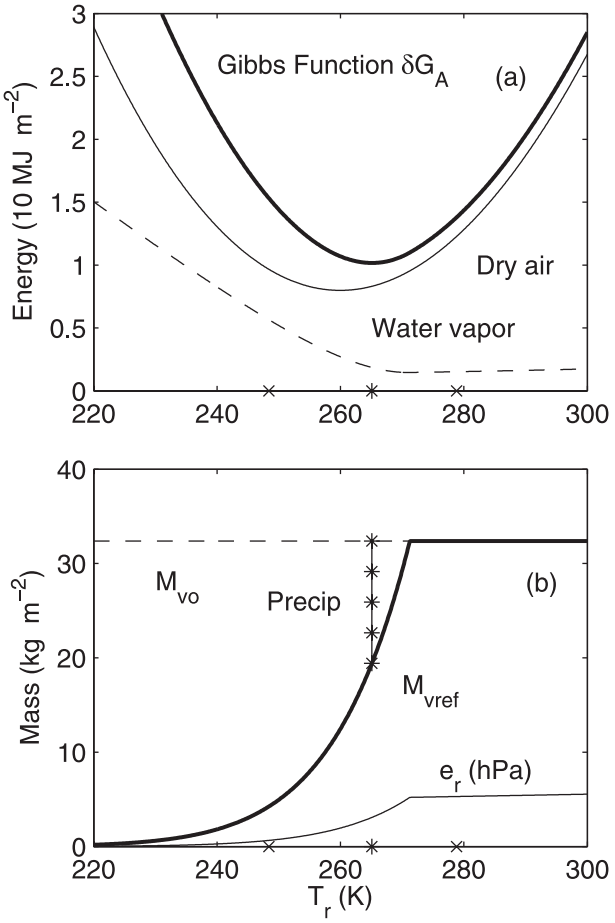

FIG. 5. (a) The atmospheric Gibbs function δG_A for the moist baroclinic zone as a function of the reference temperature T_r. The thick solid, solid, and dashed curves denote the total, dry air, and water vapor contributions. (b) The thick solid curve denotes the mass of water vapor M_{vr} in the reference atmosphere as a function of T_r. The horizontal dashed line is the mass of water vapor M_v in the atmosphere. Their difference, $M_v - M_{vr}$, denotes the amount of water in the atmosphere precipitated into the water reservoir in the reference state. The reference surface vapor pressure e_*, denoted by the thin solid curve, increases with T_r following the Clausius–Clapeyron relation until the reference atmosphere is sufficiently warm to contain all the atmosphere's water in a subsaturated state. The asterisks on the abscissas denote the equilibrium temperature $T_0 = 265.12$ K; the crosses denote the minimum and maximum equilibrium temperature of individual soundings in the ensemble.

TABLE 7. Available baroclinic energetics of the idealized baroclinic zones with horizontal temperature gradient $\Delta T_y = 30$ K. The total change in the topography cases is 3 km.

Case	T_0 (K)	$T_{\min}$ (K)	$T_{\max}$ (K)	AE (MJ m^{-2})	ABE min/max (MJ m^{-2})	LAPE (MJ m^{-2})
Poleward	254.8	231.9	274.7	6.23	5.37/3.84	2.64
No mountain	259.9	245.7	274.7	7.98	2.56/2.63	3.56
Equatorward	252.5	245.7	261.2	4.82	0.47/0.75	2.70
Moist, no mountain	265.1	248.4	278.8	10.17	5.15/3.62	—

exhibits a bimodal distribution with the potential dominating the elastic contribution. In contrast, the water vapor AE (Table 8) is dominated by the elastic contribution. This result implies that the vapor pressure perturbations dominate the potential temperature perturbations (section 4b). The water vapor AE (Fig. 7b) is also bimodal but with a thick 200-hPa layer of near-zero AE. This minimum reflects the impact of the low dewpoints between 700 and 500 hPa in the sounding (Fig. 6). The AE may be compared to the convective available potential energy by dividing by the total mass of the sounding $M_0 = 6.845 \times 10^4$ kg m^{-2}, yielding a CAPE of 1541 J kg^{-1}.

A second case is phase III of the Global Atmospheric Research Program Atlantic Tropical Experiment (GATE) sounding analyzed by Randall and Wang (1992; see their Table 1 for the ''given sounding''). This tropical sounding (Fig. 8) is relatively moist with the temperature profile close to the saturated adiabat of 70°C. This structure suggests a small value of CAPE. In contrast, the AE analysis of Table 9 and Fig. 9 indicates that the sounding is a potentially large source of kinetic energy. The general features of the AE profiles are consistent with those for the extratropical VORTEX2 sounding. These include a bimodal vertical distribution, a dominant potential contribution by the dry air, and a dominant elastic contribution by the water vapor. With a total mass of $M_0 = 9.135 \times 10^4$ kg m^{-2}, the bulk CAPE is 2212 J kg^{-1}. In contrast, Randall and Wang estimate their GCAPE to be 11 J kg^{-1}.

6. Global available energy and the general circulation

The general energy equation (4.15) is readily decomposed into components for the available and kinetic energies. Integration of the kinetic energy equation (4.6) globally over the volume of the atmosphere yields, using the divergence theorem where **n** is the unit outward normal,

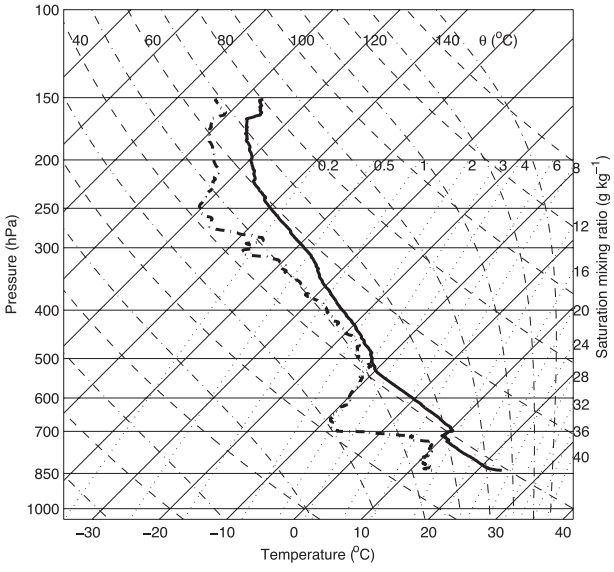

FIG. 6. Skew T–log$p$ diagram for the VORTEX2 sounding with the thick solid and dashed–dotted curves denoting the temperature and dewpoint temperature, respectively.

$$\frac{\partial \mathrm{KE}}{\partial t} = \dot{C}_{\mathrm{AE}\to\mathrm{KE}} - \dot{D}, \tag{6.1}$$

where the rate of conversion of available energy into kinetic is

$$\dot{C}_{\mathrm{AE}\to\mathrm{KE}} = \int_{V_{\mathrm{atm}}} (-\mathbf{v}\cdot\nabla p - \rho\mathbf{v}\cdot\nabla\Phi)\, dV, \tag{6.2}$$

and the integral is over the volume of the atmosphere. This conversion term indicates that flows down the pressure and geopotential gradients are kinetic energy producing. The rate of dissipation of kinetic energy is

$$\dot{D} = \int_{V_{\mathrm{atm}}} \rho\phi\, dV + \int_{A_e} (\mathbf{v}\cdot\tau + \rho \mathrm{ke}\mathbf{v})\cdot\mathbf{n}\, dA \tag{6.3}$$

and includes both interior and surface contributions. Here A_e is the surface area of the earth. In a steady state, the conversion to KE balances the dissipation of KE.

TABLE 8. Available energetics of the VORTEX2 sounding. The equilibrium temperature is $T_0 = 262.1$ K, and a surface vapor pressure $e_* = 2.4$ hPa. The ice reservoir is 6.35×10^{-5} m thick. The total AE divided by the mass of the sounding yields a CAPE of 1541 J kg^{-1}.

Component	AE (MJ m^{-2})	APE (MJ m^{-2})	AEE (MJ m^{-2})
Dry air	8.98	8.75	0.23
Water vapor	1.80	0.31	1.49
Total	10.79	9.06	1.72

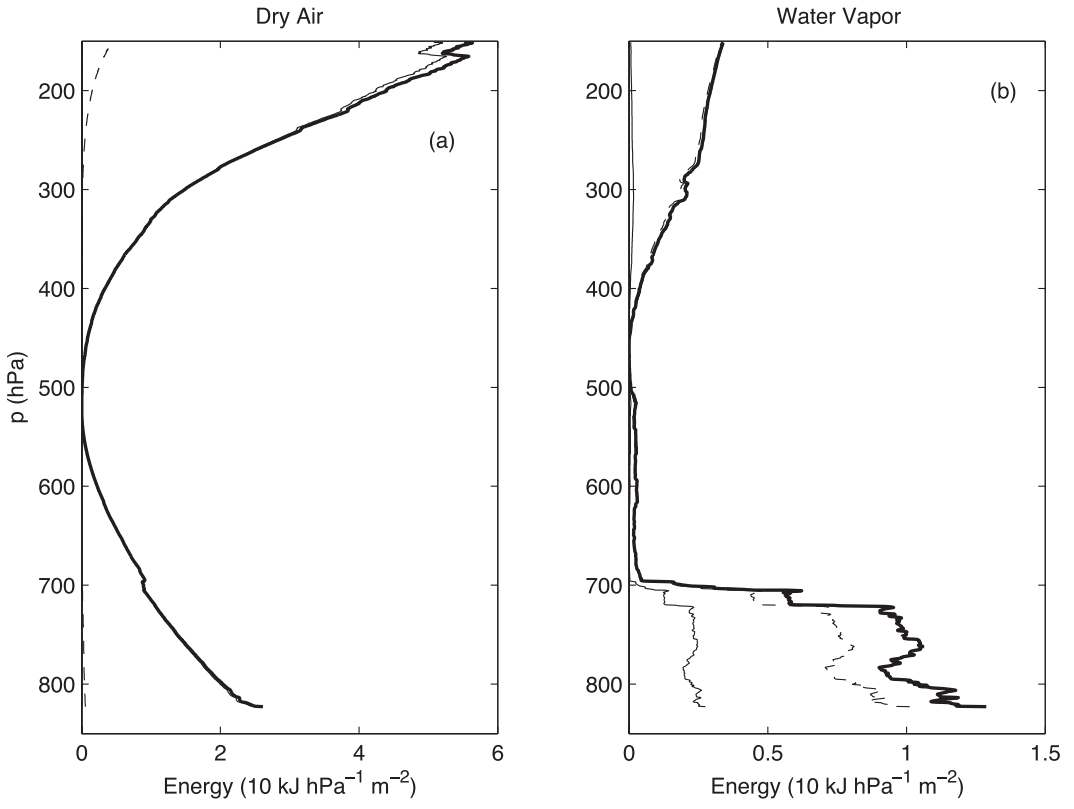

FIG. 7. Available energy for the (a) dry air and (b) water vapor as a function of pressure for the VORTEX2 sounding. The total, potential, and elastic contributions are denoted by the thick solid, solid, and dashed curves, respectively, for each component.

The global available energy equation is then

$$\frac{\partial}{\partial t}\mathrm{AE} = \dot{G} - \dot{C}_{\mathrm{AE}\to\mathrm{KE}} - T_0\dot{S}_{\mathrm{irr}}, \tag{6.4}$$

where the generation rate of available energy is

$$\dot{G} = \int_{V_{\mathrm{atm}}} \left(\frac{T - T_0}{T}\right)\rho(\dot{q} + \phi)\, dV - \int_{A_e} \rho \mathrm{ex}\mathbf{v}\cdot\mathbf{n}\, dA. \tag{6.5}$$

In a steady state, the generation by interior diabatic processes and the surface exergy flux balances the sum of the conversion to kinetic energy and the loss $T_0\dot{S}_{\mathrm{irr}} > 0$ associated with irreversible entropy production. It is noted that the energy equations (6.1)–(6.5) may be readily divided into zonally symmetric and asymmetric components. Estimates of the various processes are presented to quantify the available energy cycle for the atmosphere.

Quantification requires the determination of the equilibrium temperature T_0 for the atmosphere. Analysis of the 25-km-deep standard atmosphere with a 70% surface relative humidity and 3 km water vapor scale height yields an equilibrium temperature of 256 K with an available energy of 14 MJ m^{-2}. A more definitive determination requires analysis of a global

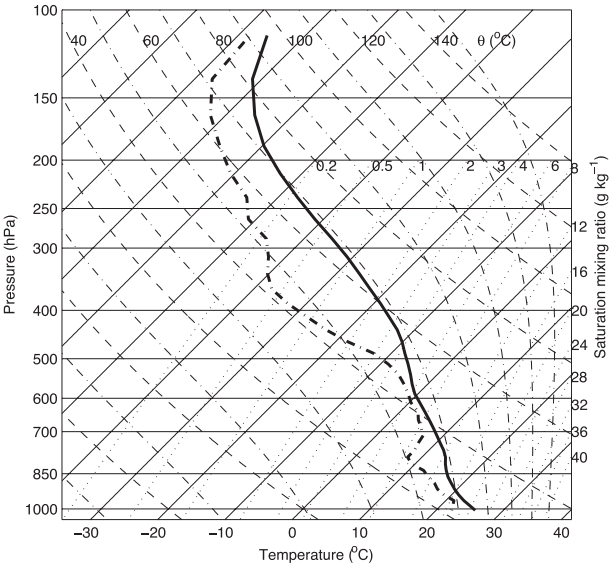

FIG. 8. As in fig. 6, but for the GATE III sounding.

TABLE 9. Available energetics of the GATE Phase III sounding. The equilibrium temperature is $T_0 = 271.4$ K with $e_* = 5.3$ hPa. The ice reservoir is 14.47×10^{-5} m thick. The total AE divided by the mass of the sounding yields a CAPE of 2212 J kg^{-1}.

Component	AE (MJ m^{-2})	APE (MJ m^{-2})	AEE (MJ m^{-2})
Dry air	16.32	15.92	0.40
Water vapor	4.40	0.68	3.73
Total	20.72	16.59	4.13

dataset. Such a calculation is beyond the scope of the current investigation. For definiteness in the following discussion, we take $T_0 = 255$ K, the planetary/effective temperature.

a. Dissipation of kinetic energy

The dissipation term (6.3) includes three distinct processes: viscous dissipation of kinetic energy within the atmosphere and the surface flux of kinetic energy out of the atmosphere by the surface wind stresses and by the precipitation of hydrometeors.

1) INTERNAL DISSIPATION

The loss due to friction can be decomposed into one due to the clear air and one due to hydrometeor drag:

$$\dot{D}_{\text{viscous}} = \int_{V_{\text{atm}}} \rho\phi_{\text{air}}\, dV, \quad \dot{D}_h = \int_{V_{\text{atm}}} \rho\phi_h\, dV. \tag{6.6}$$

Peixoto and Oort (1991) estimate the large-scale dissipation to be about 2 W m^{-2} globally. For the tropics Pauluis et al. (2000) estimate the turbulent cascade by convection to be 1 W m^{-2} and the hydrometeor dissipation to be 2–4 W m^{-2}. Using satellite data, Pauluis and Dias (2012) estimate the dissipation to be 1.8 W m^{-2}. In the extratropics there is a reduction in precipitation and a lowering of the mean height of hydrometeor formation. Globally we take the hydrometeor dissipation to be 1–3 W m^{-2}.

2) KINETIC ENERGY LOSS DUE TO PRECIPITATION

Falling hydrometeors will carry their kinetic energy out of the atmosphere at the rate

$$\dot{D}_{\text{precip}} = \int_{A_e} (\rho_h \text{ke}_h \mathbf{v}_h) \cdot \mathbf{n}\, dA \simeq \rho_h \overline{P}\, \overline{\text{ke}}_h A_e, \tag{6.7}$$

where P is the precipitation rate, $A_e = 5.1 \times 10^{14}$ m^2 is the surface area of the earth, and the subscript h denotes a hydrometeor. The overbar denotes a representative mean. For a fall speed of 1 m s^{-1} and a precipitation

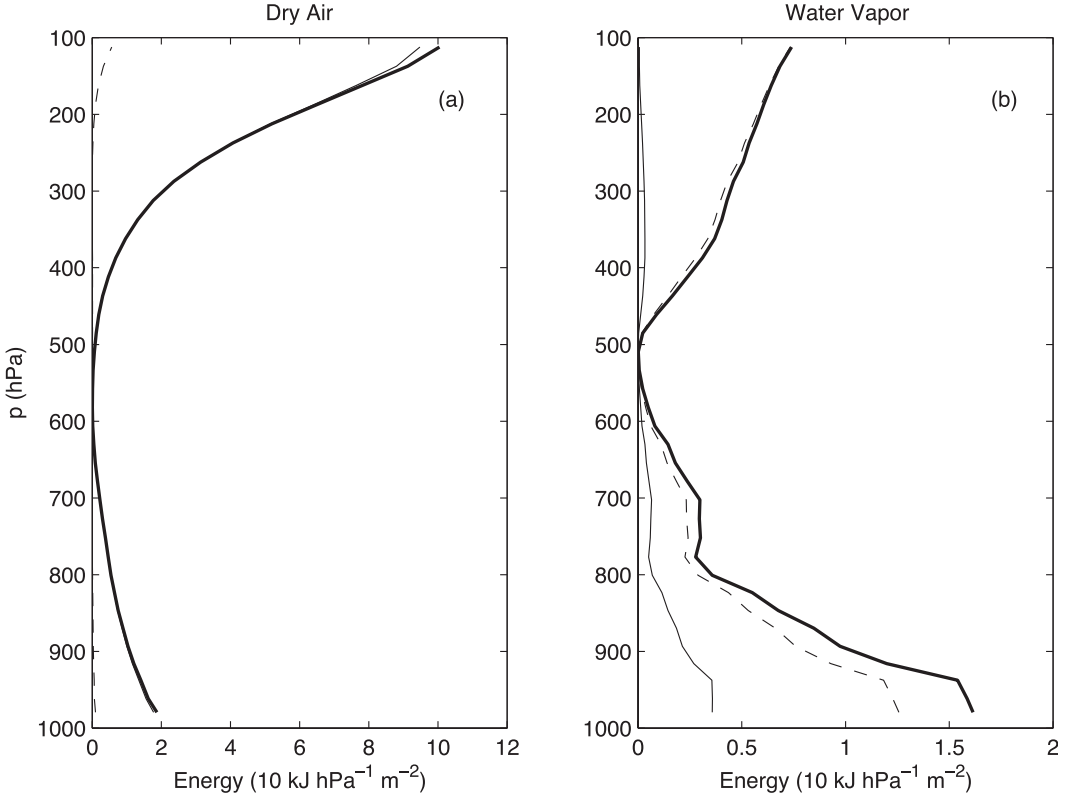

FIG. 9. As in fig. 7, but for the GATE III sounding.

TABLE 10. Dissipation of kinetic energy. In a steady state the total dissipation rate equals the rate of conversion of available energy to kinetic energy.

Process	Rate (W m^{-2})
Large-scale dissipation	2
Mesoscale dissipation	1
Hydrometeor dissipation	1–3
Wind stress	1
Precipitation	10^{-5}
Total	5–7

rate of 1 m yr^{-1} ($\rho_h \overline{P} = 3.17 \times 10^{-5}$ kg m^{-2} s^{-1}), (6.7) yields $\dot{D}_{\text{precip}} \simeq 1.59 \times 10^{-5}\,\text{W m}^{-2} A_e$.

3) KINETIC ENERGY LOSS DUE TO WIND STRESS

With surface wind speeds exceeding that of the underlying surface, there is a downward transport of kinetic energy out of the atmosphere given by $\dot{D}_{\text{stress}} = \int_{A_{\text{surface}}} \mathbf{v} \cdot \boldsymbol{\tau} \cdot \mathbf{n}\, dA$. For a surface wind of 10 m s^{-1} and bulk aerodynamic drag formulations with a drag coefficient of 10^{-3}, the downward transport is $\dot{D}_{\text{stress}} \approx \overline{v}\,\overline{\rho} C_D \overline{v^2} A_e = 1\,\text{W m}^{-2} A_e$.

Thus, the total dissipation rate is about 5–7 W m^{-2}. Table 10 summarizes the discussion.

b. Generation of available energy

The generation rate (6.5) includes surface fluxes of exergy into the atmosphere and interior diabatic processes. The interior terms are weighted by the efficiency factor $N \equiv (T - T_0)/T$ that modulates the impact of a particular process in enhancing the available energy relative to the equilibrium isothermal atmosphere (Fig. 1) at the temperature T_0. A contour plot (not shown) of the efficiency factor would have a zero contour along the $T_0 = 255$ K isotherm that runs from the middle tropical troposphere downward toward the poles (with additional zero isopleths in the upper stratosphere and lower mesosphere). For the same magnitude temperature difference ($|T - T_o|$), the efficiency would be greater above the zero isotherm than below. For example, at the surface of the tropics $N \approx (300 - 255)/300 = 15\%$, while at the polar tropopause the efficiency is $N \approx (200 - 255)/200 = -28\%$. Endothermic processes below the zero contour where the efficiency is positive would increase the available energy; exothermic processes above would also increase it.

1) RADIATION

The radiative generation of available energy is

$$\dot{G}_{\text{radiatve}} = \int_{V_{\text{atm}}} \left(\frac{T - T_0}{T}\right) \rho \dot{q}_{\text{rad}}\, dV = \int_{V_{\text{atm}}} \left(\frac{T - T_0}{T}\right) \rho c_v \dot{T}_{\text{radiative}}\, dz\, dA, \tag{6.8}$$

where the heating rate is expressed in terms of a warming rate $\dot{T}_{\text{radiative}} \approx -1$ K day^{-1}. The sum of the clear-sky shortwave and longwave warming is relatively constant with height. Then

$$\dot{G}_{\text{radiative}} \simeq \overline{\rho}_0 c_v \overline{\dot{T}}_{\text{radiative}} H_s \overline{N} A_e, \tag{6.9}$$

where the scale height is $H_s = 8$ km and $\overline{N}$ is a nondimensional integrated efficiency factor weighted by the exponential decay of density with height:

$$\overline{N} = \frac{1}{H_s} \int_0^{z_{\text{trop}}} \left(\frac{T_* - \Gamma z - T_0}{T_* - \Gamma z}\right) e^{-z/H_s}\, dz, \tag{6.10}$$

where T_* is the surface temperature and the lapse rate is $\Gamma = 6.5$ K km^{-1}. This mean efficiency varies from $\overline{N} = 2.1\%$ for the tropics ($T_* = 300$ K and $z_{\text{trop}} = 16$ km) to 0.5% for midlatitudes ($T_* = 288$ K and $z_{\text{trop}} = 12$ km) to -1.2% for the polar regions ($T_* = 273$ K and $z_{\text{trop}} = 8$ km). Then, for a mean $\overline{N} = 1\%$, the radiative processes contribute $\dot{G}_{\text{radiative}} \simeq -0.66\,\text{W m}^{-2} A_e$.

The effect of clouds on the radiative generation could be significant. Low-level cloud bases, where the efficiency is positive generally, absorb longwave radiation emitted from the surface, leading to a positive AE generation. Emission of longwave radiation to space from high-level cloud tops, where the efficiency is negative, will also generate positive AE.

2) DISSIPATION

There is a feedback of the viscous dissipation (in which kinetic energy is converted into thermal energy) to act as an available energy generation process. Assuming that all of the conversion occurs close to the surface in the boundary layer, then the feedback is positive with a maximum positive efficiency. One finds

$$\dot{G}_{\text{viscous}} = \int_{V_{\text{atm}}} \left(\frac{T - T_0}{T}\right) \rho(\phi_{\text{air}} + \phi_h)\, dV \le \left(\frac{T_* - T_0}{T_*}\right) \int_{V_{\text{atm}}} \rho(\phi_{\text{air}} + \phi_h)\, dV = \left(\frac{T_* - T_0}{T_*}\right) (5\,\text{W m}^{-2}) A_e = \frac{33}{288} (5\,\text{W m}^{-2}) A_e = 0.57\,\text{W m}^{-2} A_e. \tag{6.11}$$

3) PRECIPITATION EXERGY FLUX

The generation of exergy by precipitation is

$$\dot{G}_{\text{precipitation}} = -\int_{A_e} \rho_h P \text{ex}_h \, dA = -\rho_h \overline{\text{ex}}_h \overline{P} A_e, \quad (6.12)$$

where again $\rho_h \overline{P} = 3.17 \times 10^{-5}\,\text{kg m}^{-2}\,\text{s}^{-1}$. The exergy for liquid or solid water ($j = 3$ or 4) is

$$\text{ex}_j = \delta h_j - T_0 \delta s_j + \Phi_j = c_j T_0 [\delta \hat{T} - \ln(1 + \delta \hat{T})] + \Phi_j. \quad (6.13)$$

Because exergy is a positive definite quantity, precipitation always carries exergy out of the atmosphere and thus acts as a sink of AE. Taking $\widehat{\delta T} \simeq (288 - 255)/255 = 0.13$, the liquid water exergy is $8.28 \times 10^3\,\text{J kg}^{-1}$. The geopotential contribution in (6.13) arises from the definition (3.8). The mean continental elevation is about 1 km but land covers only 30% of the earth's surface, so $g\overline{z} \simeq 3.00 \times 10^3\,\text{J kg}^{-1}$ globally. Then, the precipitation flux is $\simeq -0.36\,\text{W m}^{-2}$. We note that the exergy of ice is about half that of liquid precipitation and that the geopotential contribution can be significant locally.

4) EVAPORATION EXERGY FLUX

The evaporation exergy generation (e.g., Pauluis 2007) is

$$\begin{aligned}\dot{G}_{\text{evaporation}} &= \int_{A_e} \rho_v E \text{ex}_v \, dA \dot{G}_E \\ &\simeq \rho_h \overline{P} \left[\text{ex}_l + \frac{T - T_0}{T} l_v(T) \right. \\ &\quad \left. + R_v T_0 \ln\left(\frac{H}{H_0}\right) \right] A_e, \end{aligned} \quad (6.14)$$

where the net evaporation is taken to equal the net precipitation and H is the relative humidity. This input is composed of three contributions. The first cancels the precipitation sink (to first order) but without the geopotential term:

$$\begin{aligned}\dot{G}_{\text{evaporation}} &\simeq \overline{\rho_v E} c_l T_0 [\delta \hat{T} - \ln(1 + \delta \hat{T})] A_e \\ &= 0.263\,\text{W m}^{-2} A_e. \end{aligned} \quad (6.15)$$

The second is due to the enthalpy of evaporation:

$$\dot{G}_{\text{evaporation}} \simeq \overline{\rho_v E} \left(\frac{T - T_0}{T} \right) l_v(T) A_e = 9.08\,\text{W m}^{-2} A_e. \quad (6.16)$$

The third is

$$\dot{G}_{\text{evaporation}} \simeq \overline{\rho_v E} R_v T_0 \ln\left(\frac{H}{H_0}\right) A_e = -2.59\,\text{W m}^{-2} A_e, \quad (6.17)$$

for $H = 50\%$ and $H_0 = 100\%$. Then the total evaporative generation is $6.75\,\text{W m}^{-2} A_e$.

5) DRY AIR EXERGY FLUX

The turbulent transport of exergy from the surface may be estimated in a manner analogous to that for the enthalpy. The bulk aerodynamic formula for the surface enthalpy flux is $F_h = \rho_a C_H |\mathbf{u}| c_{pa} T]_a^s$, where the right-hand bracket on the temperature denotes a difference across the interface between the air and the underlying surface. For a mean enthalpy flux of $24\,\text{W m}^{-2}$ (Trenberth et al. 2009), the mean air – surface temperature difference is $T]_a^s = F_h/(\rho_a C_H |\mathbf{u}| c_{pa}) = 2.4\,\text{K}$ using $C_H = 10^{-3}$. By analogy, the exergy flux is defined by $F_{\text{ex}} = \rho_a C_{\text{ex}} |\mathbf{u}| \text{ex}_a]_a^s$, where the exergy for dry air is

$$\begin{aligned}\text{ex}_a &= \delta h_a - T_0 \delta s_a = c_{pa}(T - T_0) - c_{pa} T_0 \ln\left(\frac{\theta}{\theta_0}\right) \\ &\simeq c_{pa} T_0 [\delta \hat{T} - \ln(1 + \delta \hat{\theta})] \simeq \frac{1}{2} c_{pa} T_0 (\delta \hat{T})^2. \end{aligned} \quad (6.18)$$

Near the surface $\delta \hat{\theta} \simeq \delta \hat{T}$ because the dry air pressures of the atmosphere and its equilibrium atmosphere are, to a very good approximation, equal to each other. Then, using the mean air – surface temperature difference estimated above, one finds, using $C_{\text{ex}} = 10^{-3}$, $(\delta \hat{T})^2]_a^s = (35.4^2 - 33^2)/255^2 = 2.52 \times 10^{-3}$ and $\dot{G}_{\text{ex}} = F_{\text{ex}} A_e = 3.23\,\text{W m}^{-2} A_e$.

c. Irreversible entropy production

The last term in (6.4) represents irreversible entropy production processes (e.g., the subcloud evaporation of raindrops). It is positive definite and hence is a sink of available energy. The term $T_0 \dot{S}_{\text{irr}} > 0$ is called lost work in exergy theory (e.g., Bejan 1997). Pauluis and Held (2002) estimate an irreversible entropy production of $8\,\text{W m}^{-2}$ that includes a surface contribution due to irreversible evaporation. The latter process is contained here in the third contribution of the surface evaporation (6.17). Thus, we take $T_0 \dot{S}_{\text{irr}} \approx 5.41\,\text{W m}^{-2}$.

Table 11 summarizes the discussion on the available energy generation budget.

7. Conclusions

Minimization of an atmospheric Gibbs function has been utilized to determine the temperature T_0 of an

TABLE 11. Generation of available energy. In a steady state, the total rate of generation of available energy less the lost work equals the rate of conversion of available energy to kinetic energy.

Process	Rate (W m^{-2})
Evaporation exergy flux	6.8
Dry exergy flux	3.2
Dissipation	<0.6
Radiation	−0.7
Precipitation	−0.4
Subtotal	9.5
Lost work	3.5
Total	6

isothermal equilibrium atmosphere that contains the least total energy (i.e., the sum of the internal and potential energies) of a given atmosphere obtainable by reversible processes. The difference in the total energy of the atmosphere and this equilibrium atmosphere is the maximum energy that can be converted into kinetic energy. That maximum is defined as the available energy of the atmosphere. The approach has been demonstrated for a variety of cases including moist processes and topography. In general, the available energy increases monotonically; the equilibrium temperature T_0 decreases as the depth, baroclinity, and strength of the surface easterlies increase. The inclusion of moisture and terrain sloping with the isentropes increases both the available energy and the equilibrium temperature. The available energy AE is shown to be positive definite and the sum of available potential (APE) and elastic (AEE) contributions. The available energy can also be approximately partitioned into available baroclinic energy (ABE) and available convective energy (ACE). The formalism of section 2 is completely general. It readily adapts itself to the oceanic case of a two-component geophysical fluid with an isothermal, isohaline reference ocean in hydrostatic balance. The approach may, in principle, also be applied to the earth system as a whole.

The analysis of the available energy cycle of the general circulation in section 6 is summarized in Fig. 10 and

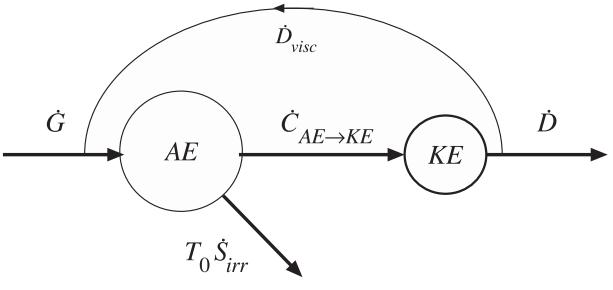

FIG. 10. Schematic diagram of the available energy cycle of the global atmosphere.

TABLE 12. Estimates of the available energy cycle of the global atmosphere.

AE (MJ m^{-2})	KE (MJ m^{-2})	$\dot{G}$ (W m^{-2})	$T_0\dot{S}_{\rm irr}$ (W m^{-2})	$\dot{C}_{A\to K}$ (W m^{-2})	$\dot{D}$ (W m^{-2})
~15	~1–2	9.5	3.5	6	6

quantified in Table 12. A measure of the efficiency η of the cycle is the ratio of the conversion rate to the generation rate. One finds $\eta = \dot{C}_{A\to K}/\dot{G} \sim 63\%$. In comparison, Karlsson (1990) estimated an efficiency of 41% for a 5-day global European Centre for Medium-Range Weather Forecasts (ECMWF) forecast. More definitive quantification of these processes is clearly needed.

Acknowledgments. The author benefited from suggestions from colleagues John A. Dutton, Dennis Lamb, Sukyoung Lee, Paul M. Markowski, and Raymond G. Najjar. Paul M. Markowski provided the VORTEX2 sounding. The comments of Olivier Pauluis and an anonymous reviewer also helped improve the manuscript.

APPENDIX A

Thermodynamics

The thermodynamic formulations are standard (e.g., Bohren and Albrecht 1998). The dry air and water vapor are treated as ideal gases with constant specific heats. The ice and liquid water are taken to be incompressible with constant specific heats. The enthalpies of phase change vary linearly with temperature following Kirchhoff's law. This dependence is included in the Clausius–Clapeyron equations for the equilibrium vapor pressures. Table A1 summarizes the notation and values of various constants.

TABLE A1. Physical constants.

Parameter	Value
Acceleration due to gravity	$g = 9.81$ m s^{-2}
Gas constant of dry air	$R = 287$ J kg^{-1} K^{-1}
Gas constant of vapor	$R_v = 461.5$ J kg^{-1} K^{-1}
Specific heat of dry air at constant pressure	$c_p = 1004$ J kg^{-1} K^{-1}
Specific heat of vapor at constant pressure	$c_{pv} = 1885$ J kg^{-1} K^{-1}
Specific heat of liquid water	$c_l = 4218$ J kg^{-1} K^{-1}
Specific heat of ice	$c_i = 2106$ J kg^{-1} K^{-1}
Enthalpy of vaporization at 0°C	$l_0 = 2.5003 \times 10^6$ J kg^{-1}
Enthalpy of fusion at 0°C	$l_f = 0.334 \times 10^6$ J kg^{-1}
Reference pressure	$p_{00} = 1000$ hPa
Triple-point temperature	$T_{\rm tp} = 273.16$ K
Triple-point pressure	$e_{\rm tp} = 6.11$ hPa

APPENDIX B

Asymmetric Chemical Potentials

This appendix assesses the impact of using equilibrium chemical potentials for the liquid and solid water without the geopotential term $-gz$ in (3.8). Then (4.8) retains the last term in (4.5) to become

$$\frac{D(\mathrm{ae}+\mathrm{ke})}{Dt}=\delta T\frac{Ds}{Dt}+\delta\mu_j\frac{D\chi_j}{Dt}+\alpha\mathbf{v}\cdot(\nabla\cdot\sigma)-\alpha\nabla\cdot(\delta p\mathbf{v})-\delta\chi_j\frac{D\mu_{0,j}}{Dt}. \tag{B.1}$$

The last term in (B.1) arises from the asymmetry in the potentials. It is

$$-\delta\chi_j\frac{D\mu_{0,j}}{Dt}=-\sum_{j=1}^{4}\delta\chi_j\frac{D\mu_{0,j}}{Dt}=-\sum_{j=1}^{2}\delta\chi_j\frac{D(-gz)}{Dt}=-\frac{D(-gz)}{Dt}\sum_{j=1}^{2}\chi_j+\frac{D(-gz)}{Dt}\sum_{j=1}^{2}\chi_{0,j}=-\frac{D(-gz)}{Dt}(1-\chi_3-\chi_4)$$
$$+\frac{D(-gz)}{Dt}=(\chi_3+\chi_4)\frac{D(-gz)}{Dt}=\frac{D(-gz)(\chi_3+\chi_4)}{Dt}-(-gz)\frac{D(\chi_3+\chi_4)}{Dt}, \tag{B.2}$$

where the chemical potentials for liquid and solid water ($j = 3, 4$) are now constants, while those for dry air and water vapor ($j = 1, 2$) are each a constant $-gz$. In addition the concentrations for the atmosphere and for the equilibrium atmosphere independently sum to unity with $\chi_{0,3\mathrm{or}4} = 0$ above the surface water reservoir. Then, the two terms on the rhs of (B.2) can be subsumed into (B.1) by modifying the potentials for liquid water and ice to include contributions due to gravity. Then, one may write (B.1) as

$$\frac{D(\mathrm{ae}'+\mathrm{ke})}{Dt}=\delta T\frac{Ds}{Dt}+\delta\mu'_j\frac{D\chi_j}{Dt}+\alpha\mathbf{v}\cdot(\nabla\cdot\sigma)-\alpha\nabla\cdot(\delta p\mathbf{v}), \tag{B.3}$$

where $\mathrm{ae}' = \delta h - T_0\delta s - \alpha\delta p - \mu'_{0,j}\delta\chi_j$, with $\mu'_{0,j} = \mu_{0,j} - gz\delta_{jk\geq 3}$. The expression (B.3) is isomorphic with (4.8) and justifies the a priori use of (3.8). Then the remainder of the derivation of (4.11) holds with the source term (4.12) becoming

$$\mathrm{sae}=\frac{\delta T}{T}\dot{q}-\frac{T_0}{T}\phi+T_0\left(\frac{\mu_j}{T}-\frac{\mu'_{0,j}}{T_0}\right)\dot{\chi}_j \tag{B.4}$$

or, using the modified potentials,

$$\mathrm{sae}=\frac{\delta T}{T}\dot{q}-\frac{T_0}{T}\phi-T_0(s_j-s'_{0,j})\dot{\chi}_j, \tag{B.5}$$

where $s'_{0,j} = s_{0,j} + (gz/T_0)\delta_{jk\geq 3}$. For example, in the case of a phase change between water vapor and liquid water we have

$$\mathrm{sae}_{\mathrm{phase}}=-T_0(s_j-s_{0,j}-gz\delta_{jk\geq 3})\dot{r}_j=-T_0R_v\ln H\dot{r}_2, \tag{B.6}$$

where H is the relative humidity. Thus, inclusion of the geopotential term in the equilibrium chemical potentials (3.8) handles entropy production during phase changes appropriately.

APPENDIX C

Idealized Baroclinic Zones

Idealized dry baroclinic zones are constructed with inspiration from the model of Eady (1949) but for a compressible atmosphere. The geometry is Cartesian with (y, z) indicating meridional and vertical coordinates. The central sounding is that for the standard atmosphere as are the lapse rates. The surface temperature varies linearly over the domain with a total variation of ΔT_y. The surface pressure is either isobaric at 1013.25 hPa or includes a horizontal gradient corresponding to a mean geostrophic zonal wind U_0 with constant Coriolis parameter of 10^{-4} s^{-1}. The pressure and density are determined from the hydrostatic relation and the ideal gas law. This construction is applied over a 6×10^3 km $\times$ 12 km grid $[-y_0 \leq y \leq y_0, z_b(y) \leq z \leq z_{\mathrm{top}}]$. Here $y_0 = 3 \times 10^3$ km and $z_{\mathrm{top}} =$ 12 km. The resolution is 100 m in the vertical and 100 km in the horizontal direction.

The topography is $z_b(y) = (z_0/2)(y/y_0 \pm 1)$ and varies linearly by z_0 over the $2y_0$ domain. The plus sign indicates topography that is a maximum at the high latitude $y = y_0$ (henceforth, the poleward case) and the minus sign one that is maximum at the low latitude $y = -y_0$ (henceforth, the equatorward case).

The effects of moisture on the baroclinic isolated jet are assessed by including a water vapor field that has a relative humidity of 70% at the surface with a scale height of 3 km. Then, the warmer lower latitudes will have greater moisture content than those at higher latitudes.

REFERENCES

Bannon, P. R., 2005: Eulerian available energetics in moist atmospheres. *J. Atmos. Sci.,* **62,** 4238–4252.

Bejan, A., 1997: *Advanced Engineering Thermodynamics.* 2nd ed. Wiley, 850 pp.

Bohren, C. F., and B. A. Albrecht, 1998: *Atmospheric Thermodynamics.* Oxford, 402 pp.

Dutton, J. A., 1973: The global thermodynamics of atmospheric motion. *Tellus,* **25,** 89–110.

——, and D. R. Johnson, 1967: The theory of available potential energy and a variational approach to atmospheric energetics. *Advances in Geophysics,* Vol. 12, Academic Press, 333–436.

Eady, E. T., 1949: Long waves and cyclone waves. *Tellus,* **1,** 33–52.

Gibbs, J. W., 1873: On the equilibrium of heterogeneous substances. *Trans. Conn. Acad. Arts Sci.,* **3,** 108–248.

——, 1874: On the equilibrium of heterogeneous substances. *Trans. Conn. Acad. Arts Sci.,* **3,** 343–524.

Karlsson, S., 1990: Energy, entropy and exergy in the atmosphere. Ph.D. thesis, Institute of Physical Resource Theory, Chalmers University of Technology, 121 pp.

Kucharski, F., 1997: On the concept of exergy and available potential energy. *Quart. J. Roy. Meteor. Soc.,* **123,** 2141–2156.

Livezey, R. E., and J. A. Dutton, 1976: The entropic energy of geophysical fluid systems. *Tellus,* **28,** 138–157.

Lorenz, E. N., 1955: Available potential energy and the maintenance of the general circulation. *Tellus,* **7,** 157–167.

——, 1967: *The Nature and Theory of the General Circulation.* WMO Press, 161 pp.

——, 1979: Numerical evaluation of moist available energy. *Tellus,* **31,** 230–235.

Margules, M., 1910: On the energy of storms. *Smithson. Misc. Collect.,* **51,** 533–595.

Mechoso, C. R., 1980: Baroclinic instability of lows along sloping boundaries. *J. Atmos. Sci.,* **37,** 1393–1399.

Pauluis, O., 2007: Sources and sinks of available potential energy in a moist atmosphere. *J. Atmos. Sci.,* **64,** 2627–2641.

——, and I. M. Held, 2002: Entropy budget of an atmosphere in radiative–convective equilibrium. Part I: Maximum work and frictional dissipation. *J. Atmos. Sci.,* **59,** 125–139.

——, and J. Dias, 2012: Satellite estimates of precipitation-induced dissipation in the atmosphere. *Science,* **335,** 953–956.

——, V. Balaji, and I. M. Held, 2000: Frictional dissipation in a precipitating atmosphere. *J. Atmos. Sci.,* **57,** 989–994.

Peixoto, J. P., and A. H. Oort, 1991: *Physics of Climate.* American Institute of Physics, 564 pp.

Randall, D. A., and J. Wang, 1992: The moist available energy of a conditionally unstable atmosphere. *J. Atmos. Sci.,* **49,** 240–255.

Reif, F., 1965: *Fundamentals of Statistical and Thermal Physics.* McGraw-Hill, 651 pp.

Trenberth, K. E., J. T. Fasullo, and J. Kiehl, 2009: Earth's global energy budget. *Bull. Amer. Meteor. Soc.,* **90,** 311–323.